

# Structural and Spectroscopic Evidence for Intramolecular Agostic $M\cdots H-C$ and Dative $Zr\leftarrow F-C(\text{ortho})$ Interactions in the Zwitterionic Metal Complexes $[(C_5H_4)SiMe_2(N-t-Bu)]M(+)(\mu-C_4H_6)B(-)(C_6F_5)_3$ , $M = Ti, Zr$

Frithjof Hannig,<sup>1a</sup> Roland Fröhlich,<sup>1a</sup> Klaus Bergander,<sup>1a</sup> Gerhard Erker,<sup>1a</sup> and Jeffrey L. Petersen<sup>\*,1b</sup>

Organisch-Chemisches Institut der Universität Münster, Corrensstrasse 40, D-48149 Münster, Germany, and C. Eugene Bennett Department of Chemistry, West Virginia University, Morgantown, West Virginia 26506-6045

Received April 22, 2004

The reactions of equimolar amounts of  $[(C_5H_4)SiMe_2(N-t-Bu)]M(C_4H_6)$  ( $M = Ti, Zr$ ) and  $B(C_6F_5)_3$  proceed cleanly with the formation of the zwitterionic complexes  $[(C_5H_4)SiMe_2(N-t-Bu)]M(+)(\mu-C_4H_6)B(-)(C_6F_5)_3$ . X-ray structural analyses of these novel compounds indicate that the  $\pi$ -allyl unit within the asymmetrical bridging *cis*-butadiene moiety adopts the *Z*-configuration. The structure of the zwitterionic Ti-betaine complex is stabilized by a pair of  $Ti(+)\cdots H-CB(-)$  agostic interactions, whereas the structure of the Zr analogue features a dative  $Zr\leftarrow F-C(\text{ortho})$  interaction with a  $Zr-F$  distance of 2.324(1) Å and a single  $Zr(+)\cdots H-CB(-)$  agostic interaction. Variable-temperature  $^{19}F$  NMR data show that the broad ortho-F resonance for the three freely rotating perfluorophenyl groups at room temperature separates upon cooling (193 K) to produce six distinct signals at  $\delta$  -124.8, -129.6, -131.8, -133.4, -135.7, and -189.2, consistent with the coordination of an ortho-F atom to the electrophilic Zr center. From a line shape analysis the free energy barrier for disruption of this  $Zr\leftarrow F-C(\text{ortho})$  interaction is estimated to be ca. 9.8 kcal/mol ( $T_c = 223$  K).

## Introduction

Homogeneous olefin polymerization catalysts may be generated by the treatment of group 4 organometal dimethyl or butadiene complexes with a strong Lewis acid, such as  $B(C_6F_5)_3$ . In the former case,  $B(C_6F_5)_3$  abstracts a methyl ligand to give the borate anion  $[BMe(C_6F_5)_3]^-$  and the catalytically active organometal methyl cation. Structural studies of borate salts of various zirconocenium methyl cations<sup>2–6</sup> have subsequently revealed that these  $[Cp_2ZrMe][BMe(C_6F_5)_3]$ -type ion-pairs are stabilized by a  $Zr(+)\cdots Me-B(-)$  interaction, in which the methyl group acts as a bridge between the positively charged Zr and the negatively charged boron. In contrast, the addition of a stoichiometric amount of  $B(C_6F_5)_3$  to group 4 metallocene butadiene complexes takes place regioselectively to afford zwitterionic metal

betaine complexes<sup>7</sup> in which the boron is covalently tethered to a terminal carbon of the coordinated butadiene fragment, leaving a distorted  $\pi$ -allyl functionality bound to the metal. Variable-temperature  $^{19}F$  NMR experiments performed on  $Cp_2Zr(+)(\mu-C_4H_6)B(-)(C_6F_5)_3$ <sup>7a</sup> and several related Zr-betaine complexes<sup>7c,g</sup> revealed that in solution the electrophilic zirconium center is protected by a weak  $Zr\leftarrow F-C(\text{ortho})$  interaction involving a  $C_6F_5$  ring. This dative  $Zr-F$  interaction was confirmed in the solid state for  $Cp_2Zr(+)(\mu-C_4H_6)B(-)(C_6F_5)_3$ ,<sup>7a</sup>  $(C_5H_4Me)_2Zr(+)(\mu-C_4H_6)B(-)(C_6F_5)_3$ ,<sup>7c</sup>  $Cp_2Zr(+)(\mu-CH_2CMeCHCH_2)B(-)(C_6F_5)_3$ ,<sup>7c</sup>  $[Me_2Si(1-indenyl)_2]Zr(+)(\mu-C_4H_6)B(-)(C_6F_5)_3$ ,<sup>7f</sup>  $[Me_2Si(C_5H_4)_2]Zr(+)(\mu-C_4H_6)B(-)(C_6F_5)_3$ ,<sup>7g</sup> and  $[Me_2Si(3-MeC_5H_3)_2]Zr(+)(\mu-C_4H_6)B(-)(C_6F_5)_3$ ,<sup>7g</sup> but was not observed for the sterically crowded zwitterion  $(C_5Me_5)_2Zr(+)(\mu-C_4H_6)B(-)(C_6F_5)_3$ <sup>7d</sup> or in the mixed-ring ansa-zirconocene zwitterions  $[Me_2C(C_5H_4)(indenyl)]Zr(+)(\mu-C_4H_6)B(-)(C_6F_5)_3$ <sup>7g</sup> and  $[Me_2C(C_5H_4)(fluorenyl)]Zr(+)(\mu-C_4H_6)B(-)(C_6F_5)_3$ .<sup>7g</sup>

With the development of “constrained-geometry” catalysts derived from  $[(C_5R_4)SiMe_2(NR')]ML_2$ -type com-

\* To whom correspondence should be addressed. E-mail: jpetersen@vuu.edu.

(1) (a) University of Münster. (b) West Virginia University.

(2) (a) Yang, X.; Stern, C. L.; Marks, T. J. *J. Am. Chem. Soc.* **1991**, *113*, 3623. (b) Yang, X.; Stern, C. L.; Marks, T. J. *J. Am. Chem. Soc.* **1994**, *116*, 10015.

(3) Bochmann, M.; Lancaster, S. J.; Hursthouse, M. B.; Abdul Malik, K. M. *Organometallics* **1994**, *13*, 2235.

(4) (a) Beck, S.; Prosenic, M. H.; Brintzinger, H. H.; Goretzki, R.; Herfert, N.; Fink, G. J. *Mol. Catal. A: Chem.* **1996**, *111*, 67. (b) Beck, S.; Lieber, S.; Schaper, F.; Geyer, A.; Brintzinger, H. H. *J. Am. Chem. Soc.* **2001**, *123*, 1483.

(5) Guzei, I. A.; Stockland, R. A., Jr.; Jordan, R. F. *Acta Crystallogr., Sect. C* **2000**, *56*, 635.

(6) Liu, Z.; Somsok, E.; Landis, C. R. *J. Am. Chem. Soc.* **2001**, *123*, 2915.

(7) (a) Temme, B.; Erker, G.; Karl, J.; Luftmann, H.; Fröhlich, R.; Kotila, S. *Angew. Chem., Int. Ed. Engl.* **1995**, *34*, 1755. (b) Temme, B.; Karl, J.; Erker, G. *Chem. Eur. J.* **1996**, *2*, 919. (c) Karl, J.; Erker, G.; Fröhlich, R. *J. Am. Chem. Soc.* **1997**, *119*, 11165. (d) Karl, J.; Erker, G.; Fröhlich, R. *J. Organomet. Chem.* **1997**, *535*, 59. (e) Karl, J.; Dahlmann, M.; Erker, G.; Bergander, K. *J. Am. Chem. Soc.* **1998**, *120*, 5643. (f) Dahlmann, M.; Erker, G.; Nissinen, M.; Fröhlich, R. *J. Am. Chem. Soc.* **1999**, *121*, 2820. (g) Dahlmann, M.; Erker, G.; Fröhlich, R.; Meyer, O. *Organometallics*, **2000**, *19*, 2956.

plexes,<sup>8–10</sup> researchers at The Dow Chemical Company in collaboration with Marks and co-workers<sup>11</sup> prepared several Ti diene complexes, [(C<sub>5</sub>Me<sub>4</sub>)SiMe<sub>2</sub>(NR<sup>1</sup>)]Ti-(R<sup>2</sup>CHCHCHR<sup>3</sup>), where R<sup>1</sup> = t-Bu, C<sub>6</sub>H<sub>5</sub>; R<sup>2</sup> = H, Me; R<sup>3</sup> = H, Me. These highly electrophilic Ti diene complexes when activated with MAO, (HNMe<sub>2</sub>Ph)[B(C<sub>6</sub>F<sub>5</sub>)<sub>4</sub>], or B(C<sub>6</sub>F<sub>5</sub>)<sub>3</sub> afford highly active homogeneous catalysts. Jones, Cowley, and co-workers<sup>12</sup> have prepared several zwitterionic group 4 metal complexes by the stoichiometric treatment of [(C<sub>5</sub>Me<sub>4</sub>)SiMe<sub>2</sub>(N-t-Bu)]M(diene) complexes (M = Ti, Zr) with B(C<sub>6</sub>F<sub>5</sub>)<sub>3</sub> and Al(C<sub>6</sub>F<sub>5</sub>)<sub>3</sub>. Their structural analyses of [(C<sub>5</sub>Me<sub>4</sub>)SiMe<sub>2</sub>(N-t-Bu)]M(+)(μ-CH(Me)CHCH<sub>2</sub>)B(-)(C<sub>6</sub>F<sub>5</sub>)<sub>3</sub> confirmed that the B(C<sub>6</sub>F<sub>5</sub>)<sub>3</sub> unit is attached to the terminal CH<sub>2</sub> group of the pentadiene and provided direct evidence for the presence of a pair of agostic M(+)...H-CB(-) interactions. The solution <sup>19</sup>F NMR spectra exhibited by these zwitterionic complexes, however, gave no indication of a M-F-C(ortho) interaction upon cooling.

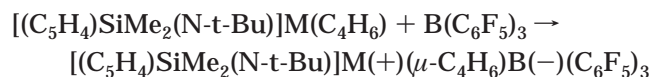
The available structural data show that the type of ancillary cyclopentadienyl ligand in these zwitterionic systems has a dramatic effect on the internal conformational structure of the bridging butadiene unit. For the zwitterionic zirconocene systems<sup>7</sup> both the *E* (transoid) and the *Z* (cisoid) configuration have been observed. Alternatively, the X-ray structural analyses of [(C<sub>5</sub>Me<sub>4</sub>)SiMe<sub>2</sub>(N-t-Bu)]M(+)(μ-CH(Me)CHCH<sub>2</sub>)B(-)(C<sub>6</sub>F<sub>5</sub>)<sub>3</sub> and related zwitterionic complexes<sup>12</sup> revealed that the bridging butadiene consistently exhibits the *Z*-configuration. This arrangement directs the two hydrogen atoms of the terminal B-bound CH<sub>2</sub> group of the diene toward the electrophilic metal center and thereby blocks the possibility of an intramolecular M-F-C(ortho) interaction.<sup>7g,12</sup>

Recently, we reported the preparation and structural characterization of butadiene derivatives of [(C<sub>5</sub>H<sub>4</sub>)SiMe<sub>2</sub>(N-t-Bu)]MCl<sub>2</sub>, M = Ti, Zr.<sup>13</sup> Although [(C<sub>5</sub>H<sub>4</sub>)SiMe<sub>2</sub>(N-t-Bu)]Ti(η<sup>4</sup>-C<sub>4</sub>H<sub>6</sub>)<sup>13</sup> and [(C<sub>5</sub>Me<sub>4</sub>)SiMe<sub>2</sub>(N-t-Bu)]Ti(η<sup>4</sup>-CH(Me)CHCH<sub>2</sub>)<sup>11</sup> exhibit analogous “prone” structures, the solid structures of [(C<sub>5</sub>H<sub>4</sub>)SiMe<sub>2</sub>(N-t-Bu)]Zr(C<sub>4</sub>H<sub>6</sub>) and related ansa-permethylocyclopentadienyl-amido Zr butadiene complexes<sup>13,14</sup> are dramatically different. Whereas these latter Zr butadiene complexes are monomeric, the solid state structure of [(C<sub>5</sub>H<sub>4</sub>)SiMe<sub>2</sub>(N-t-Bu)]Zr(C<sub>4</sub>H<sub>6</sub>) is tetranuclear with each pair of Zr centers linked by an unsymmetrically bridging butadiene via an unusual (1,2,3-η<sup>3</sup>)-Zr-(4-μ<sub>2</sub>)-Zr bonding interaction. This structural difference prompted us to investigate the stereochemical influence of the sterically less demanding and weaker π-donating cyclopentadienyl ring on the molecular structures and spectroscopic properties exhibited by the zwitterionic complexes [(C<sub>5</sub>H<sub>4</sub>)SiMe<sub>2</sub>(N-t-Bu)]M(+)(μ-C<sub>4</sub>H<sub>6</sub>)B(-)(C<sub>6</sub>F<sub>5</sub>)<sub>3</sub> derived

from [(C<sub>5</sub>H<sub>4</sub>)SiMe<sub>2</sub>(N-t-Bu)]M(C<sub>4</sub>H<sub>6</sub>), M = Ti, Zr. The results of our investigations are reported herein and provide structural and spectroscopic evidence for the existence of intramolecular agostic M(+)...H-CB(-) and Zr-F-C(ortho) interactions in these systems.

## Discussion of Results

**Preparation and Characterization of Electrophilic Zwitterionic [(C<sub>5</sub>H<sub>4</sub>)SiMe<sub>2</sub>(N-t-Bu)]M(+)(μ-C<sub>4</sub>H<sub>6</sub>)B(-)(C<sub>6</sub>F<sub>5</sub>)<sub>3</sub> (M = Ti, Zr) Complexes.** Equimolar amounts of [(C<sub>5</sub>H<sub>4</sub>)SiMe<sub>2</sub>(N-t-Bu)]M(C<sub>4</sub>H<sub>6</sub>) (M = Ti, Zr) and B(C<sub>6</sub>F<sub>5</sub>)<sub>3</sub> react to produce only the zwitterionic metal betaine complexes [(C<sub>5</sub>H<sub>4</sub>)SiMe<sub>2</sub>(N-t-Bu)]M(+)(μ-C<sub>4</sub>H<sub>6</sub>)B(-)(C<sub>6</sub>F<sub>5</sub>)<sub>3</sub>. These compounds were characterized



in solution by multinuclear (<sup>1</sup>H, <sup>11</sup>B, <sup>13</sup>C, <sup>19</sup>F) NMR measurements. The formation of a dative bond between a terminal carbon of the butadiene fragment and the boron produces four distinct resonances for the proximal and distal protons and carbons of the cyclopentadienyl ring and yields two signals for the methyl protons and carbons of the SiMe<sub>2</sub> linkage. The six protons and the four carbons of the butadiene fragment become chemically inequivalent. In the Ti-betaine complex the six butadiene protons appear as two multiplets at δ 2.68 and 2.63 for the protons of the CH<sub>2</sub> attached to the cationic titanium center, as a pair of multiplets centered at δ 4.96 and 4.15 for the protons of the two internal CH units, and as a pair of broad upfield resonances at δ 0.65 and -0.80 for the protons of the CH<sub>2</sub> bound to the anionic boron atom. The butadiene carbon resonances are observed at δ 75.6 for the terminal butadiene carbon bound to Ti, at δ 127.1 and 110.0 for the two internal butadiene carbons, and as a broad signal at δ 26.2 for the carbon bound to the boron. For the Zr-betaine complex the two multiplets at δ 2.38 and 1.15 are assigned to the two inequivalent protons of the CH<sub>2</sub> attached to the cationic zirconium center, the downfield multiplet centered at δ 6.42 corresponds to the proton of the internal CH closest to Zr, the broad signal at δ 5.03 is assigned to the proton of the internal CH closest to B, and the two broad signals at δ 0.90 and -0.38 represent the protons of the CH<sub>2</sub> bound to the anionic boron atom. The terminal butadiene carbons bound to Zr and B are located at δ 65.7 and 21.5, respectively, with the two internal carbons found at δ 145.6 and 117.6, respectively.

At room temperature the three C<sub>6</sub>F<sub>5</sub> groups attached to the boron in these zwitterionic complexes are freely rotating. Their <sup>13</sup>C NMR spectra contain three characteristic downfield doublets for the ortho-, meta-, and para-carbons of the perfluorophenyl groups. The <sup>19</sup>F NMR spectrum of [(C<sub>5</sub>H<sub>4</sub>)SiMe<sub>2</sub>(N-t-Bu)]Ti(+)(μ-C<sub>4</sub>H<sub>6</sub>)B(-)(C<sub>6</sub>F<sub>5</sub>)<sub>3</sub> exhibits a doublet at δ -131.9, a triplet at δ -159.2, and a triplet at δ -164.2 for the ortho-, para-, and meta-F atoms, respectively. In contrast, in the ambient <sup>19</sup>F NMR spectrum of [(C<sub>5</sub>H<sub>4</sub>)SiMe<sub>2</sub>(N-t-Bu)]Zr(+)(μ-C<sub>4</sub>H<sub>6</sub>)B(-)(C<sub>6</sub>F<sub>5</sub>)<sub>3</sub>, the ortho-F atoms display a broad signal at δ -140.6, whereas the meta- and para-F atoms give two apparent *singlets* at δ -159.2 and -163.8, respectively, indicative of dynamical behavior

(8) Shapiro, P. J.; Bunel, E.; Schaefer, W. P.; Bercaw, J. E. *Organometallics* **1990**, *9*, 867.

(9) Stevens, J. C.; Timmers, F. J.; Rosen, G. W.; Knight, G. W.; Lai, S. Y. Eur. Patent Appl. EP 0 416-815 A2, 1991.

(10) Canich, J. M. Eur. Patent Appl. EP 0 420 436 A1, 1991.

(11) Devore, D. D.; Timmers, F. J.; Hasha, D. L.; Rosen, R. K.; Marks, T. J.; Deck, P. A.; Stern, C. L. *Organometallics* **1995**, *14*, 3132.

(12) (a) Cowley, A. H.; Hair, G. S.; McBurnett, B. G.; Jones, R. A. *J. Chem. Soc., Chem. Commun.* **1999**, 437. (b) Hair, G. S.; Jones, R. A.; Cowley, A. H.; Lynch, V. *Inorg. Chem.* **2001**, *40*, 1014.

(13) Strauch, J. W.; Petersen, J. L. *Organometallics* **2001**, *20*, 2623.

(14) Dahlmann, M.; Schottek, J.; Fröhlich, R.; Kunz, D.; Nissinen, M.; Erker, G.; Fink, G.; Kleinschmidt, R. *J. Chem. Soc., Dalton Trans.* **2000**, 1881.

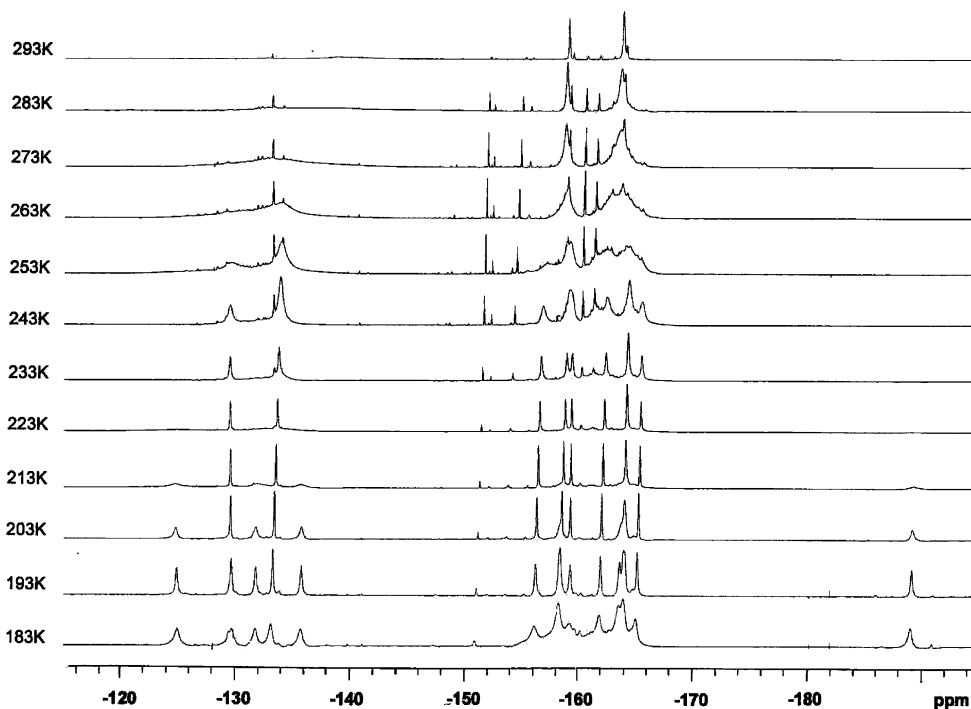


**Figure 1.** Variable-temperature  $^{19}\text{F}$  NMR spectra measured from 183 to 298 K for  $[(\text{C}_5\text{H}_4)\text{SiMe}_2(\text{N-t-Bu})]\text{Zr}(+)(\mu\text{-C}_4\text{H}_6)\text{B}(-)(\text{C}_6\text{F}_5)_3$  in toluene- $d_8$ .

in solution. Further evidence was provided by the cooling of a toluene- $d_8$  solution of  $[(\text{C}_5\text{H}_4)\text{SiMe}_2(\text{N-t-Bu})]\text{Zr}(+)(\mu\text{-C}_4\text{H}_6)\text{B}(-)(\text{C}_6\text{F}_5)_3$  from 293 to 183 K (Figure 1). The broad ortho-F signal observed at 293 K eventually produces five signals at  $\delta$   $-124.8$ ,  $-129.6$ ,  $-131.8$ ,  $-133.4$ , and  $-135.7$  and a sixth one shifted dramatically upfield to  $\delta$   $-189.2$ , consistent with dative coordination of an ortho-fluorine atom to zirconium.<sup>7a,c,g</sup> The para-F and meta-F signals also broaden and split into seven resolved resonances at  $\delta$   $-156.3$ ,  $-158.4$  (2F),  $-159.2$ ,  $-161.9$ ,  $-163.6$ ,  $-164.0$  (2F), and  $-165.1$ . The variable-temperature  $^{19}\text{F}$  NMR data reveal that the evolution of the six ortho-F signals occurs in two stages, in a manner similar to the 1:1 Lewis acid–base adduct of  $\text{B}(\text{C}_6\text{F}_5)_3$  and 1-methylbenzimidazole.<sup>15</sup> The two signals at  $\delta$   $-129.6$  and  $-133.4$  for one of the  $\text{C}_6\text{F}_5$  rings begin to sharpen at 233 K, whereas the remaining four ortho-F signals emerge as broad resonances below 223 K and then sharpen at 193 K. This behavior indicates that one  $\text{C}_6\text{F}_5$  ring adopts a spatial orientation whereby its two ortho-F nuclei become diastereotopic on the NMR time scale. Upon F-coordination, the four remaining ortho-F nuclei become conformationally locked with the signal of the Zr-bound F found upfield.

The free energy activation barrier for disruption of the dative  $\text{Zr}\leftarrow\text{F}\text{-C}(\text{ortho})$  interaction was estimated from the variation in the line widths of these four  $^{19}\text{F}$  NMR resonances in the spectra measured at 193, 203, and 213 K. The fitting of their NMR spectral line shapes was performed with the aid of the DNMR (4-spin) routine within the simulation program WINDNMR.<sup>16</sup>

The observed intensities and line widths of these four resonances are effectively equal (Figure 1). The contribution to the inherent line width in the absence of exchange at each temperature was estimated from the line widths of the two ortho-F resonances at  $\delta$   $-129.6$  and  $-133.4$ , which are not exchanging below 223 K. As the temperature decreases from 213 K, the observed broadening of these two signals reflects the increase in the solution's viscosity. The corresponding rate constants obtained from the line shape simulation were found to be  $45\text{ s}^{-1}$  (193 K),  $155\text{ s}^{-1}$  (203 K), and  $425\text{ s}^{-1}$  (213 K). From an Eyring plot, the calculated values of  $\Delta H^\ddagger$  and  $\Delta S^\ddagger$  obtained from the least-squares fit ( $R^2 = 0.999$ ) gave  $\Delta G^\ddagger = 9.8 \pm 0.5\text{ kcal/mol}$  at  $T_c = 223\text{ K}$ . This value is comparable to the range of 8–10 kcal/mol (Table 1) for the intramolecular  $\text{Zr}\leftarrow\text{F}\text{-C}(\text{ortho})$  interactions in  $\text{Cp}_2\text{Zr}(+)(\mu\text{-C}_4\text{H}_6)\text{B}(-)(\text{C}_6\text{F}_5)_3$  and several related zwitterionic zirconocene complexes.<sup>7a,c,g</sup>

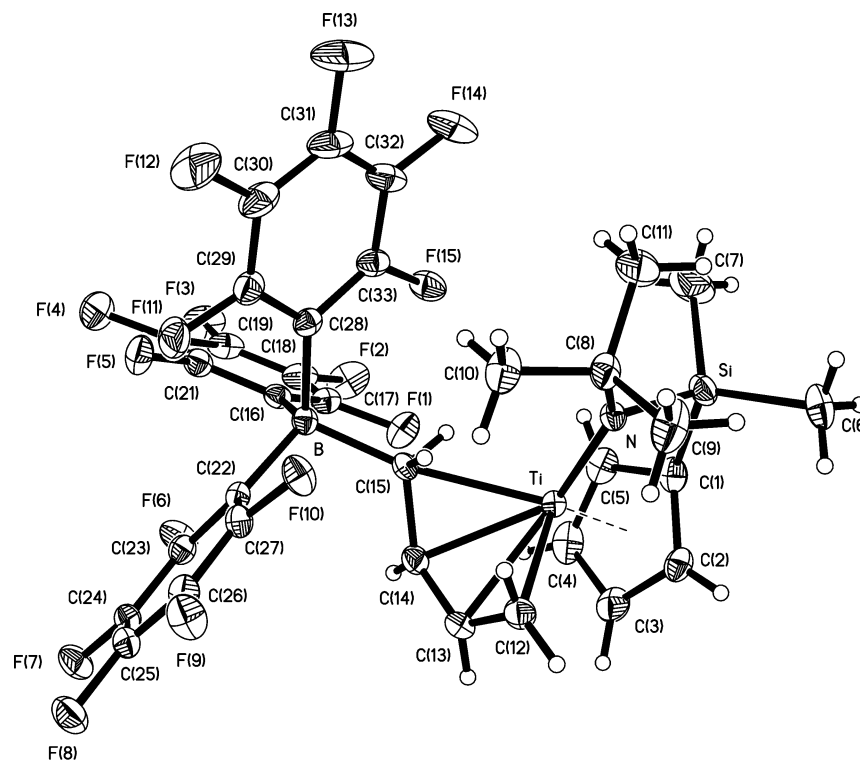
**Molecular Structure of  $[(\text{C}_5\text{H}_4)\text{SiMe}_2(\text{N-t-Bu})]\text{Ti}(+)(\mu\text{-C}_4\text{H}_6)\text{B}(-)(\text{C}_6\text{F}_5)_3$ .** The molecular structure of  $[(\text{C}_5\text{H}_4)\text{SiMe}_2(\text{N-t-Bu})]\text{Ti}(+)(\mu\text{-C}_4\text{H}_6)\text{B}(-)(\text{C}_6\text{F}_5)_3$  was determined from the analysis of X-ray diffraction data collected at  $-50\text{ }^\circ\text{C}$ . The perspective view of the molecular structure, which is displayed in Figure 2 with the atom-labeling scheme, shows that carbon C(15) is bound to B, producing a slightly bent  $\text{Ti}\text{-C}(15)\text{-B}$  bond angle of  $169.4(2)^\circ$ . The  $\text{B}\text{-C}(15)$  bond of  $1.683(3)\text{ \AA}$  is noticeably longer than the three  $\text{B}\text{-C}(\text{C}_6\text{F}_5)$  bonds that range from  $1.644(3)$  to  $1.661(3)\text{ \AA}$ . Although all four carbons of the butadiene moiety remain bound to Ti, the four  $\text{Ti}\text{-C}$  bonds ( $\text{Ti}\text{-C}(12)$ ,  $2.204(3)$ ;  $\text{Ti}\text{-C}(13)$ ,  $2.342(3)$ ;  $\text{Ti}\text{-C}(14)$ ,  $2.311(2)$ ;  $\text{Ti}\text{-C}(15)$ ,  $2.332(2)\text{ \AA}$ ) reflect an asymmetric coordination of the butadiene unit, with C(15) being  $0.13\text{ \AA}$  farther than C(12) from the electrophilic Ti atom. The conversion of  $[(\text{C}_5\text{H}_4)\text{SiMe}_2(\text{N-t-Bu})]\text{Ti}(\text{C}_4\text{H}_6)$  to  $[(\text{C}_5\text{H}_4)\text{SiMe}_2(\text{N-t-Bu})]\text{Ti}(+)(\mu\text{-C}_4\text{H}_6)\text{B}(-)(\text{C}_6\text{F}_5)_3$  is accompanied by modest reductions in the  $\text{Ti}\text{-N}$  and

(15) Vagedes, D.; Erker, G.; Kehr, G.; Bergander, K.; Kataeva, O.; Fröhlich, R.; Grimme, S.; Mück-Lichtenfeld, C. *J. Chem. Soc., Dalton Trans.* **2003**, 1337.

(16) WINDNMR (version 7.1) was obtained from Professor Hans J. Reich, Department of Chemistry, University of Wisconsin, Madison, WI 53706. This NMR spectral simulation program may be downloaded from <http://www.chem.wisc.edu/areas/reich/plt/windnmr.htm>.

**Table 1. Summary of Structural and Dynamic  $^{19}\text{F}$  NMR Data for Zwitterionic Group 4 Metal Complexes Exhibiting an Intramolecular Zr←F–C(ortho) Interaction**

compound	config	$\Delta G^\ddagger$ ( $T_c$ )	$d(\text{Zr}-\text{F})$
$\text{Cp}_2\text{Zr}(+)(\mu\text{-C}_4\text{H}_6)\text{B}(-)(\text{C}_6\text{F}_5)_3$	<i>E</i>	8.1 (233)	2.423(3)
$\text{Cp}_2\text{Hf}(+)(\mu\text{-C}_4\text{H}_6)\text{B}(-)(\text{C}_6\text{F}_5)_3$	<i>E</i>	8.0 (233)	
$(\text{C}_5\text{H}_4\text{Me})_2\text{Zr}(+)(\mu\text{-C}_4\text{H}_6)\text{B}(-)(\text{C}_6\text{F}_5)_3$	<i>E</i>	8.5 (243)	2.408(2)
$\text{Cp}_2\text{Zr}(+)(\mu\text{-CH}_2\text{CPhCHCH}_2)\text{B}(-)(\text{C}_6\text{F}_5)_3$	<i>E</i>	8.4 (243)	
$\text{Cp}_2\text{Zr}(+)(\mu\text{-CH}_2\text{CMeCHCH}_2)\text{B}(-)(\text{C}_6\text{F}_5)_3$	<i>E</i>		2.402(1)
$[\text{Me}_2\text{Si}(\text{C}_5\text{H}_4)_2]\text{Zr}(+)(\mu\text{-C}_4\text{H}_6)\text{B}(-)(\text{C}_6\text{F}_5)_3$	<i>E</i>	8.7 (250)	2.385(3)
$[\text{Me}_2\text{Si}(3\text{-MeC}_5\text{H}_3)_2]\text{Zr}(+)(\mu\text{-C}_4\text{H}_6)\text{B}(-)(\text{C}_6\text{F}_5)_3$	<i>E</i>	9.7 (275)	2.403(1)
$[\text{Me}_2\text{Si}(1\text{-indenyl})_2]\text{Zr}(+)(\mu\text{-C}_4\text{H}_6)\text{B}(-)(\text{C}_6\text{F}_5)_3$	<i>E</i>		2.483(3)
$[(\text{C}_5\text{H}_4)\text{SiMe}_2(\text{N-t-Bu})]\text{Zr}(+)(\mu\text{-C}_4\text{H}_6)\text{B}(-)(\text{C}_6\text{F}_5)_3$	<i>Z</i>	9.8 (223)	2.324(1)

**Figure 2.** Perspective view of the molecular structure of the zwitterionic Ti-betaine complex  $[(\text{C}_5\text{H}_4)\text{SiMe}_2(\text{N-t-Bu})]\text{Ti}(+)(\mu\text{-C}_4\text{H}_6)\text{B}(-)(\text{C}_6\text{F}_5)_3$  with the atom-numbering scheme. The thermal ellipsoids are scaled to enclose 30% probability.

the Ti–Cp(c) distances from 1.978(3) to 1.940(2) Å and from 2.031 to 2.016 Å, respectively.

Within the butadiene fragment, the four carbon atoms are arranged in a cis-conformation with the open end of the butadiene cup pointed away from the cyclopentadienyl ring. This spatial arrangement is analogous to that displayed by the 1,3-pentadiene linkage in  $[(\text{C}_5\text{Me}_4)\text{SiMe}_2(\text{N-t-Bu})]\text{M}(+)(\mu\text{-C}_4\text{H}_5\text{Me})\text{B}(-)(\text{C}_6\text{F}_5)_3$ .<sup>12a</sup> The C(12)–C(13), C(13)–C(14), and C(14)–C(15) bond distances within the butadiene moiety of 1.408(4), 1.380(4), and 1.486(3) Å, respectively, indicate that the formation of the dative C(15)–B bond is accompanied by an appreciable reduction in the C(14)–C(15) bond order.

The highly distorted five-coordinate geometry about C(15) consists of the Ti, B, C(14), and  $\sigma$ -bonded hydrogen atoms, H(15A) and H(15B). The acute H(15A)–C(15)–Ti and H(15B)–C(15)–Ti angles of 73.5° and 60.7°, respectively, and the short Ti⋯H(15A) and Ti⋯H(15B) distances of 2.28 and 2.03 Å, respectively, reflect the presence of a pair of Ti(+) $\cdots$ H–CB(–) agostic interactions. This structural feature was first observed by Cowley and co-workers<sup>12a</sup> in the solid state structure of  $[(\text{C}_5\text{Me}_4)\text{SiMe}_2(\text{N-t-Bu})]\text{Ti}(+)(\mu\text{-C}_4\text{H}_5\text{Me})\text{B}(-)(\text{C}_6\text{F}_5)_3$ . This

Ti-betaine complex exhibits a weak IR band at 2680  $\text{cm}^{-1}$ , which was tentatively assigned to the vibrational frequency of an agostic C–H stretch. The IR spectrum of  $[(\text{C}_5\text{H}_4)\text{SiMe}_2(\text{N-t-Bu})]\text{Ti}(+)(\mu\text{-C}_4\text{H}_6)\text{B}(-)(\text{C}_6\text{F}_5)_3$  displays a barely discernible absorption at 2670  $\text{cm}^{-1}$ .

**Molecular Structure of  $[(\text{C}_5\text{H}_4)\text{SiMe}_2(\text{N-t-Bu})]\text{Zr}(+)(\mu\text{-C}_4\text{H}_6)\text{B}(-)(\text{C}_6\text{F}_5)_3$ .** The molecular structure of  $[(\text{C}_5\text{H}_4)\text{SiMe}_2(\text{N-t-Bu})]\text{Zr}(+)(\mu\text{-C}_4\text{H}_6)\text{B}(-)(\text{C}_6\text{F}_5)_3$  was determined from X-ray diffraction data measured at –75 °C. Although the crystal lattice contains a disordered molecule of toluene, the structure of this Zr zwitterion is well-behaved. A perspective view is provided in Figure 3 with the atom-labeling scheme.

The Zr butadiene unit and boron are linked by a dative C(15)–B bond of 1.663(2) Å, and the overall molecular structure is highlighted by a dative Zr←F–C(ortho) bonding interaction. The C(12)–C(13), C(13)–C(14), and C(14)–C(15) bond distances within the butadiene moiety of 1.407(2), 1.379(2), and 1.521(2) Å, respectively, show that the formation of the C(15)–B bond leads to a substantial lengthening of the C(14)–C(15) bond. The Zr–F(1) distance of 2.324(1) Å is substantially longer than the Zr–F  $\sigma$ -bond of 1.98(1) Å in  $\text{Cp}_2\text{ZrF}_2$ <sup>17</sup> or the sum of the single bond radii for Zr

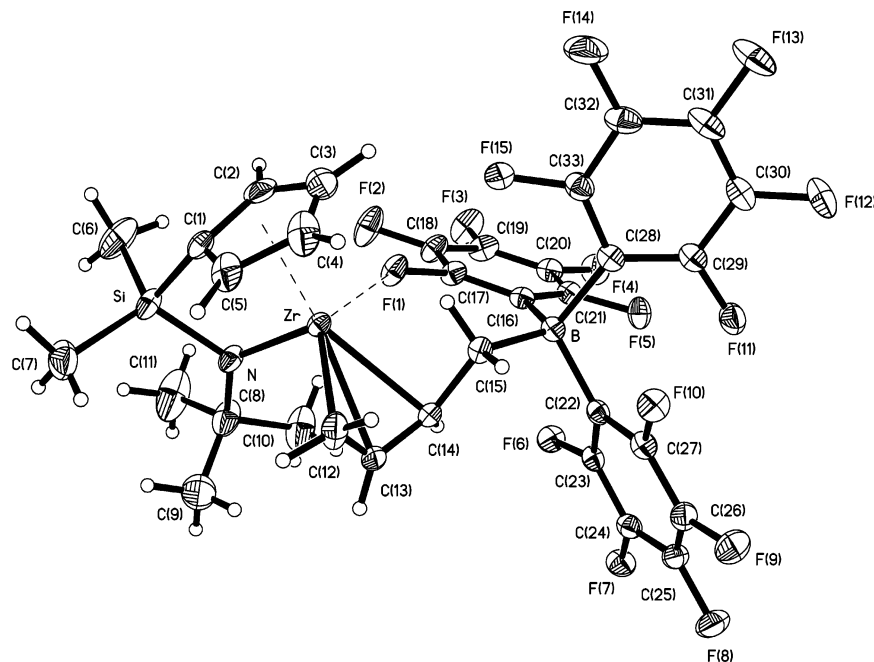


**Figure 3.** Perspective view of the molecular structure of the zwitterionic Zr-betaine complex  $[(C_5H_4)SiMe_2(N-t-Bu)]Zr(+)(\mu-C_4H_6)B(-)(C_6F_5)_3$  with the atom-numbering scheme. The thermal ellipsoids are scaled to enclose 30% probability.

(1.45 Å) and F (0.64 Å).<sup>18</sup> In comparison to other zwitterionic complexes featuring a dative intramolecular Zr–F–C(ortho) interaction, this distance lies closer to the relatively short Zr–F interatomic distances of 2.267(5) Å in  $(C_5Me_5)Zr(+)[\eta^5-C_5Me_4CH_2B(-)(C_6F_5)_3]Cl$ <sup>19</sup> and 2.310(3) Å in  $Cp_2Zr(+)[\eta^5-C_5H_4B(-)(C_6F_5)_3]$ <sup>20</sup> but falls well below the Zr–F separations ranging from 2.385(3) Å in  $[Me_2Si(C_5H_4)_2]Zr(+)(\mu-C_4H_6)B(-)(C_6F_5)_3$ <sup>7g</sup> to 2.483(3) Å in  $[Me_2Si(1-indenyl)_2]Zr(+)(\mu-C_4H_6)B(-)(C_6F_5)_3$ .<sup>7f</sup> The F(1)–C(17) of 1.398(2) Å is noticeably longer than the remaining 14 C–F bond distances, which range from 1.341(2) to 1.361(2) Å. The Zr–F(1)–C(17) angle of 151.1(1)° lies well above the relatively narrow range of 137.4–142.6° found for the zwitterionic Zr-betaine complexes featuring an intramolecular dative Zr–F–C(ortho) interaction.<sup>7</sup>

The four Zr–C(butadiene) interatomic distances (Zr–C(12), 2.347(2); Zr–C(13), 2.477(1); Zr–C(14), 2.465(1); Zr···C(15), 2.784(1) Å) indicate that the butadiene is clearly bound as an  $\eta^3$ -allyl unit. Although C(15) is not directly bonded to Zr, the Zr···H(15A) distance of 2.21 Å is consistent with the presence of a Zr···H(15A)–C(15) agostic interaction. The  $\eta^3$ -allyl moiety within  $[(C_5H_4)SiMe_2(N-t-Bu)]Zr(+)(\mu-C_4H_6)B(-)(C_6F_5)_3$  adopts the analogous *Z*-configuration observed for  $[(C_5Me_4)SiMe_2(N-t-Bu)]Zr(+)(\mu-C_4H_5Me)B(-)(C_6F_5)_3$ . However, the open end of the cup of the *cis*-butadiene fragment in the former zwitterion is directed toward the cyclopentadienyl ring, whereas in the latter case it is pointed away from the permethylated cyclopentadienyl ring.

In the zwitterionic zirconocene betaine complexes  $Cp_2Zr(+)(\mu-C_4H_6)B(-)(C_6F_5)_3$ ,<sup>7a</sup>  $(C_5H_4Me)_2Zr(+)(\mu-C_4H_6)B(-)(C_6F_5)_3$ ,<sup>7c</sup>  $Cp_2Zr(+)(\mu-CH_2CMeCH_2)B(-)(C_6F_5)_3$ ,<sup>7c</sup>

$[Me_2Si(1-indenyl)_2]Zr(+)(\mu-C_4H_6)B(-)(C_6F_5)_3$ ,<sup>7f</sup>  $[Me_2Si(C_5H_4)_2]Zr(+)(\mu-C_4H_6)B(-)(C_6F_5)_3$ ,<sup>7g</sup>  $[Me_2Si(3-MeC_5H_3)_2]Zr(+)(\mu-C_4H_6)B(-)(C_6F_5)_3$ ,<sup>7g</sup> and  $(C_5Me_5)_2Zr(+)(\mu-C_4H_6)B(-)(C_6F_5)_3$ ,<sup>7d</sup> the  $\pi$ -allyl unit consistently adopts the *E*-configuration. The two bulky  $C_5Me_5$  rings in  $(C_5Me_5)_2Zr(+)(\mu-C_4H_6)B(-)(C_6F_5)_3$  effectively direct the  $B(C_6F_5)_3$  unit away from the metallocene wedge and thereby prevent an intramolecular dative Zr–F interaction in this system. Alternatively, in the mixed-ring ansa-zirconocene zwitterions  $[Me_2C(C_5H_4)(indenyl)]Zr(+)(\mu-C_4H_6)B(-)(C_6F_5)_3$ ,<sup>7g</sup> and  $[Me_2C(C_5H_4)(fluorenyl)]Zr(+)(\mu-C_4H_6)B(-)(C_6F_5)_3$ ,<sup>7g</sup> the  $\eta^3$ -allyl moiety adopts the *Z*-configuration. In these two complexes the *cisoid* butadiene linkage is stabilized by an intramolecular Zr···C–B(–) interaction and directs the open end of the butadiene cup toward the cyclopentadienyl ring. In contrast, the X-ray structural data for the zwitterionic Ti- and Zr-betaine complexes featuring an ansa-monocyclopentadienyldimethylsilylamido ligand indicate that the  $\eta^3$ -allyl unit in these complexes consistently displays the *Z*-configuration with the open end of the butadiene cup directed either toward or away from the cyclopentadienyl functionality.<sup>12</sup> Whereas the replacement of the bulky  $C_5Me_5$  ring with the  $C_5H_4$  ring has little effect on the structures exhibited by  $[(C_5Me_4)SiMe_2(N-t-Bu)]Ti(+)(\mu-C_4H_5Me)B(-)(C_6F_5)_3$  and  $[(C_5H_4)SiMe_2(N-t-Bu)]Ti(+)(\mu-C_4H_6)B(-)(C_6F_5)_3$ , the structures of their Zr analogues are dramatically different. The greater coordinative unsaturation introduced by the weaker  $\pi$ -donating ability and smaller size of the  $C_5H_4$  ring is compensated by the formation of an intramolecular Zr–F–C(ortho) interaction that leads to an alternative orientation of the *cis*-butadiene unit in  $[(C_5H_4)SiMe_2(N-t-Bu)]Zr(+)(\mu-C_4H_6)B(-)(C_6F_5)_3$ .

## Summary

The accumulative structural data indicate that the coordinative unsaturation of the cationic metal center within these novel zwitterionic group 4 metal complexes

(17) Bush, M. A.; Sim, G. A. *J. Chem. Soc. A* **1971**, 2225.

(18) Pauling, L. *The Nature of the Chemical Bond*, 3rd ed.; Cornell Press: Ithaca, New York, 1960.

(19) Sun, Y.; Spence, R. E. v. H.; Piers, W. E.; Parvez, M.; Yap, G. P. A. *J. Am. Chem. Soc.* **1997**, *119*, 5132.

(20) Kleigrew, N.; Brackemeyer, T.; Kehr, G.; Fröhlich, R.; Erker, G. *Organometallics*, **2001**, *20*, 1952.

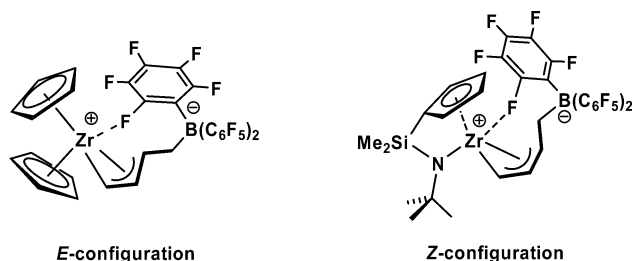


**Figure 4.** Structures depicting the *E*- and *Z*-configurations adopted by the  $\pi$ -allyl group within the bridging butadiene unit.

promotes intramolecular interactions between the electrophilic  $d^0$  metal and the terminal  $\text{CH}_2\text{B}(-)(\text{C}_6\text{F}_5)_3$  moiety. The conformation (*E* vs *Z*, Figure 4) of the  $\pi$ -allyl unit within the bridging butadiene as well as the nature (dative  $\text{Zr}\leftarrow\text{F}-\text{C}(\text{ortho})$  and/or agostic  $\text{M}(+)\cdots\text{H}-\text{CB}(-)$ ) of these stabilizing interactions are highly dependent on the type of ancillary ligand attached to the metal center. Both *E*- and *Z*-configurations have been identified for zwitterionic zirconocene complexes containing a pair of linked or unlinked cyclopentadienyl-type ligands. The *Z*-configuration is preferred for the zwitterions featuring a bifunctional ansa-monocyclopentadienyldimethylsilylamido ligand. However, as indicated in Table 1, the lateral  $\text{Zr}\leftarrow\text{F}-\text{C}(\text{ortho})$  interaction is only observed in the former Zr zwitterions when the  $\pi$ -allyl unit adopts the *E*-configuration, whereas this intramolecular stabilization arises in  $[(\text{C}_5\text{H}_4)\text{SiMe}_2(\text{N-t-Bu})\text{Zr}(+)\text{B}(-)(\text{C}_6\text{F}_5)_3]$  for the alternative *Z*-configuration.

## Experimental Section

Reagent grade hydrocarbon and ethereal solvents were purified using standard methods. Pentane and toluene were refluxed under nitrogen over Na/K and transferred to storage flasks containing  $[(\text{C}_5\text{H}_5)_2\text{Ti}(\mu\text{-Cl})_2]_2\text{Zn}$ .<sup>21</sup> Deuterated solvents were dried over activated 4 Å molecular sieves.  $[(\text{C}_5\text{H}_4)\text{SiMe}_2(\text{N-t-Bu})\text{M}(\text{C}_4\text{H}_6)]$  ( $\text{M} = \text{Ti}, \text{Zr}$ )<sup>13</sup> and  $\text{B}(\text{C}_6\text{F}_5)_3$ <sup>22</sup> were prepared by published methods. To ensure the absence of any coordinated water, a pentane solution of  $\text{B}(\text{C}_6\text{F}_5)_3$  was treated with  $\text{SiMe}_3\text{Cl}$ . Following removal of the volatiles, the water-free  $\text{B}(\text{C}_6\text{F}_5)_3$  was purified by sublimation.

All syntheses were carried out on a double-manifold high-vacuum line or under nitrogen in a Vacuum Atmospheres glovebox equipped with an HE-493 Dri-Train. Reactions were typically performed in pressure-equalizing filter frits equipped with high-vacuum Teflon stopcocks and Solv-seal joints. Nitrogen was purified by passage over reduced BTS catalyst and activated 4 Å molecular sieves. All glassware was thoroughly oven-dried and flame-dried under vacuum prior to use. NMR sample tubes were sealed under approximately 500 Torr of nitrogen.

The NMR spectra were recorded with a JEOL Eclipse 270 NMR spectrometer ( $^1\text{H}$ ,  $^{13}\text{C}$ ) at WVU or a Varian Unity 600 NMR spectrometer ( $^1\text{H}$ ,  $^{11}\text{B}$ ,  $^{13}\text{C}$ ,  $^{19}\text{F}$ ) at the University of Münster. The proton and carbon assignments were verified by the corresponding 2D COSY, HETCOR, GHSQC, and GHMBC spectra. The IR spectra were measured with a Perkin-Elmer 1600 Series FT-IR as Nujol mulls with NaCl plates. Elemental analyses were performed by Complete Analysis Laboratories Inc., E+R Microanalytical Division, Parsippany, NJ 07054.

**Preparation of  $[(\text{C}_5\text{H}_4)\text{SiMe}_2(\text{N-t-Bu})\text{Ti}(+)\text{B}(-)(\text{C}_6\text{F}_5)_3]$ .** A 115 mg sample of  $[(\text{C}_5\text{H}_4)\text{SiMe}_2(\text{N-t-Bu})\text{Ti}(\text{C}_4\text{H}_6)]$  (0.39 mmol) and 200 mg of  $\text{B}(\text{C}_6\text{F}_5)_3$  (0.39 mmol) were added

**Table 2. X-ray Crystallographic Data for the Zwitterionic Betaine Complexes  $[(\text{C}_5\text{H}_4)\text{SiMe}_2(\text{N-t-Bu})\text{M}(+)\text{B}(-)(\text{C}_6\text{F}_5)_3]$ ,  $\text{M} = \text{Ti}, \text{Zr}$**

	A. Crystal Data	$\text{C}_{40}\text{H}_{33}\text{BF}_{15}\text{NSiZr}$
emp formula	$\text{C}_{33}\text{H}_{25}\text{BF}_{15}\text{NSiTi}$	light yellow
color	dark red-brown	$0.15 \times 0.35 \times 0.40$
cryst dimens, mm	$0.32 \times 0.50 \times 0.50$	monoclinic
cryst syst	triclinic	$P2_1/c$
space group	$P\bar{1}$	14.807(1)
<i>a</i> , Å	12.028(1)	12.101(1)
<i>b</i> , Å	12.536(1)	22.507(1)
<i>c</i> , Å	13.3260(5)	90
$\alpha$ , deg	67.368(5)	93.60(1)
$\beta$ , deg	83.613(5)	90
$\gamma$ , deg	64.033(6)	4024.8(5)
volume, Å <sup>3</sup>	1663.3(3)	4
<i>Z</i>	2	942.79
fw, amu	807.34	1.556
calc density, g/cm <sup>3</sup>	1.612	4.03
$\mu$ , cm <sup>-1</sup>	4.04	1896
<i>F</i> (0 0 0)	812	198 ± 2
temperature, K	223 ± 2	
B. Data Collection and Structural Analyses		
scan type	$\omega$ , variable	CCD
scan params	4.0–10.0 deg/min	1.0 deg; 60 s frames
2 $\theta$ range, deg	3.9–52.0	3.62–55.76
2 $\theta$ range, centered reflns	10–25°	
reflns sampled	<i>h</i> (−8 ≤ <i>h</i> ≤ 14)	<i>h</i> (−19 ≤ <i>h</i> ≤ 19)
	<i>k</i> (−14 ≤ <i>k</i> ≤ 14)	<i>k</i> (−15 ≤ <i>k</i> ≤ 14)
	<i>l</i> (−16 ≤ <i>l</i> ≤ 16)	<i>l</i> (−29 ≤ <i>l</i> ≤ 29)
no. of reflns collected	6678	17 443
no. of unique data	6361 ( $R_{\text{int}} = 0.0137$ )	9584 ( $R_{\text{int}} = 0.0225$ )
no. of data, $I > 2\sigma(I)$	4858	7506
<i>R</i> indices, $I > 2\sigma(I)$	$R_1 = 0.0381$ ; $wR_2 = 0.0850$	$R_1 = 0.0390$ ; $wR_2 = 0.0949$
<i>R</i> indices, all data	$R_1 = 0.0599$ ; $wR_2 = 0.0955$	$R_1 = 0.0564$ ; $wR_2 = 0.1031$
$\sigma_1$ , GOF	1.035	1.028
weighting, <i>a</i> and <i>b</i>	0.0412, 0.6251	0.0464, 2.4490
no. of variables	492	567
max. diff peak and hole, e Å <sup>-3</sup>	0.346, −0.238	0.576, −0.321

to a 100 mL Solv-seal flask. Then 10 mL of toluene, which had been dried by storing in the presence of  $\text{Cp}_2\text{ZrMe}_2$ , was added via vacuum distillation. The reaction mixture was stirred for about 30 min at room temperature. Following the removal of the toluene, the product residue was washed with pentane and then dried under vacuo to afford a dark red-brown product. Yield: 0.257 g, 0.318 mmol (82%).

Suitable crystals of this zwitterionic Ti-betaine complex for C/H/N elemental analyses and X-ray crystallographic analysis were obtained by diffusion of the reactants toward each other using pentane as the solvent. A cylindrical tube equipped with a 15 mm Solv-seal joint and fitted with a concentric 5 mm tube was used for this purpose. Stoichiometric amounts of  $\text{B}(\text{C}_6\text{F}_5)_3$  and  $[(\text{C}_5\text{H}_4)\text{SiMe}_2(\text{N-t-Bu})]\text{Ti}(\text{C}_4\text{H}_6)$  were placed at the bottom of the larger outer and smaller inner tubes, respectively. Dry pentane was added dropwise to the reaction tube to a level of roughly 2 cm above the top of the inner tube. The Solv-seal joint was capped, and the diffusion tube was set aside with minimal agitation. After two weeks, dark crystals began to appear. Once the diffusion process had run its course, the solvent was removed, leaving large dark translucent crystals.

$^1\text{H}$  NMR (599.9 MHz, toluene- $d_6$ ):  $\delta$  5.90, 5.57, 5.46, 5.18 (s, 1H,  $\text{C}_5\text{H}_4$ ); 4.96 (m, 1H,  $\text{TiCH}_2\text{CH}$ ), 4.15 (pseudo t, 1H,  $\text{BCH}_2\text{CH}$ ), 2.68, 2.63 (m, 1H,  $\text{TiCH}_2$ ); 0.80 (s, 9H, t-Bu); 0.65 (br d, 1H,  $\text{BCH}_2$ ); 0.39, 0.15 (s, 3H,  $\text{SiMe}_2$ ); -0.80 (br s, 1H,  $\text{BCH}_2$ ).  $^{11}\text{B}$  NMR (192 MHz):  $\delta$  -12.57.  $^{13}\text{C}$  NMR (150.8 MHz,  $^1J_{\text{C-X}}$  in Hz):  $\delta$  148.6 (d, ortho C–F, 239), 139.6 (d, para C–F, 246), 137.5 (d, meta C–F, 250), 127.1 ( $\text{TiCH}_2\text{CH}$ , d, 160), 124.0 ( $\text{C}_5\text{H}_4$ , d, 176), 123.9 ( $\text{C}_5\text{H}_4$ , d, 168), 123.6 ( $\text{C}_5\text{H}_4$ , d, 176), 122 (ipso-C, br), 119.4 ( $\text{C}_5\text{H}_4$ , d, 178), 110.4 (bridgehead C, s), 110.0 ( $\text{BCH}_2\text{CH}$ , d, 168), 75.6 ( $\text{TiCH}_2$ , dd, 167, 144), 62.6 ( $\text{NCMe}_3$ , s), 33.7 ( $\text{NCMe}_3$ , q, 126), 26.2 ( $\text{BCH}_2$ , br), 1.12 ( $\text{SiMe}_2$ , q, 121).  $^{19}\text{F}$  NMR (564.3 MHz,  $^3J_{\text{F-F}}$  in Hz):  $\delta$  -131.9 (d, ortho C–F, 20), -159.2 (t, para C–F, 21), -164.2 (t, meta C–F, 19). IR ( $\text{cm}^{-1}$ ): 2954(s), 2914(s), 2853(s), 2725(w), 2670(vw), 1642(m), 1514(m), 1461(s), 1377(s), 1366(sh), 1279(m), 1256(m), 1179(m), 1087(s), 1048(m), 1016(w), 978(s), 962(sh), 921(w), 900(w), 861(w), 837(m), 797(m), 788(m), 762(m), 741(s), 722(sh), 684(m), 677(m), 663(w), 650(w). Anal. Calcd for  $\text{C}_{33}\text{H}_{25}\text{NSiBF}_{15}\text{Ti}$ : C, 49.09; H, 3.12; N, 1.73. Found: C, 49.35; H, 3.49; N, 1.71.

**Preparation of  $[(\text{C}_5\text{H}_4)\text{SiMe}_2(\text{N-t-Bu})]\text{Zr}^+(\mu\text{-C}_4\text{H}_6)\text{B}^-(\text{C}_6\text{F}_5)_3$ .** A 135.5 mg sample of  $[(\text{C}_5\text{H}_4)\text{SiMe}_2(\text{N-t-Bu})]\text{Zr}(\text{C}_4\text{H}_6)$  (0.40 mmol) and 204.8 mg of  $\text{B}(\text{C}_6\text{F}_5)_3$  (0.40 mmol) were added to a 100 mL Solv-seal flask. Following addition of 10 mL of dry toluene, the reaction mixture was stirred for about 30 min at room temperature. After removal of the toluene, the product residue was washed with pentane and then dried under vacuo to afford a light yellow solid. Yield: 0.257 g, 0.302 mmol (76%).

Suitable crystals for the X-ray structural analysis were obtained by cooling a saturated toluene solution. The sample submitted for elemental analysis was prepared by washing the crystals in pentane and then leaving the sample under high vacuum for several days.

$^1\text{H}$  NMR (599.9 MHz, toluene- $d_6$ ):  $\delta$  6.42 (m, 1H,  $\text{ZrCH}_2\text{CH}$ ), 6.40 (2 overlapping signals,  $\text{C}_5\text{H}_4$ ), 6.04, 5.78 (s, 1H,  $\text{C}_5\text{H}_4$ ), 5.03 (br s, 1H,  $\text{BCH}_2\text{CH}$ ), 2.38 (m, 1H,  $\text{ZrCH}_2$ ), 1.15 (m, 1H,  $\text{ZrCH}_2$ ), 0.90 (br d, 1H,  $\text{BCH}_2$ ), 0.75 (s, 9H, t-Bu), 0.32, 0.04 (s, 3H,  $\text{SiMe}_2$ ), -0.38 (br s, 1H,  $\text{BCH}_2$ ).  $^{11}\text{B}$  NMR (192 MHz):  $\delta$  -14.33.  $^{13}\text{C}\{^1\text{H}\}$  NMR (150.8 MHz,  $^1J_{\text{C-F}}$  in Hz):  $\delta$  149.5 (d, ortho C–F, 235), 139.3 (d, para C–F, 250), 137.5 (d, meta C–F, 252), 145.6 ( $\text{ZrCH}_2\text{CH}$ ), 123.2 (ipso-C, br), 121.0, 119.6, 118.3, 112.4 ( $\text{C}_5\text{H}_4$ ), 117.6 ( $\text{BCH}_2\text{CH}$ ), 115.7 (bridgehead C), 65.7 ( $\text{ZrCH}_2$ ), 61.2 ( $\text{NCMe}_3$ ), 34.4 ( $\text{NCMe}_3$ ), 21.5 (br,  $\text{BCH}_2$ ), 2.82, 0.02 ( $\text{SiMe}_2$ ).  $^{19}\text{F}$  NMR (562.5 MHz, 298 K):  $\delta$  -140.6 (br, ortho C–F), -159.2 (s, para C–F), -163.8 (s, meta C–F).  $^{19}\text{F}$  NMR (562.5 MHz, 193 K):  $\delta$  -124.8, -129.6, -131.8, -133.4,

**Table 3. Interatomic Distances (Å) and Bond Angles (deg) for  $[(\text{C}_5\text{H}_4)\text{SiMe}_2(\text{N-t-Bu})]\text{M}^+(\mu\text{-C}_4\text{H}_6)\text{B}^-(\text{C}_6\text{F}_5)_3$ ,  $\text{M} = \text{Ti}, \text{Zr}^a$**

A. Interatomic Distances			
Ti–N	1.940(2)	Zr–N	2.059(1)
Ti–C(1)	2.235(2)	Zr–C(1)	2.442(1)
Ti–C(2)	2.322(2)	Zr–C(2)	2.477(2)
Ti–C(3)	2.447(3)	Zr–C(3)	2.540(2)
Ti–C(4)	2.427(3)	Zr–C(4)	2.533(2)
Ti–C(5)	2.288(2)	Zr–C(5)	2.456(1)
Ti–Cp(c)	2.016	Zr–Cp(c)	2.182
Ti–C(12)	2.204(3)	Zr–C(12)	2.347(2)
Ti–C(13)	2.342(3)	Zr–C(13)	2.477(1)
Ti–C(14)	2.311(2)	Zr–C(14)	2.465(1)
Ti–C(15)	2.332(2)	Zr···C(15)	2.784(1)
Ti···H(15A) <sup>b</sup>	2.28	Zr–F(1)	2.324(1)
Ti···H(15B) <sup>b</sup>	2.03	Zr···H(15A) <sup>b</sup>	2.21
Si–N	1.772(2)	Si–N	1.765(1)
Si–C(1)	1.849(3)	Si–C(1)	1.859(2)
C(12)–C(13)	1.408(4)	C(12)–C(13)	1.407(2)
C(13)–C(14)	1.380(4)	C(13)–C(14)	1.379(2)
C(14)–C(15)	1.486(3)	C(14)–C(15)	1.521(2)
B–C(15)	1.683(3)	B–C(15)	1.663(2)
B–C(16)	1.651(3)	B–C(16)	1.659(2)
B–C(22)	1.644(3)	B–C(22)	1.658(2)
B–C(28)	1.661(3)	B–C(28)	1.665(2)
B. Bond Angles			
N–Ti–Cp(c)	110.9	N–Zr–Cp(c)	101.2
N–Ti–C(12)	101.0(1)	N–Zr–C(12)	105.1(1)
N–Ti–C(13)	133.5(1)	N–Zr–C(13)	96.9(1)
N–Ti–C(14)	137.3(1)	N–Zr–C(14)	110.1(1)
N–Ti–C(15)	104.2(1)	N–Zr–C(15)	140.8(1)
N–Si–C(1)	93.5(1)	N–Si–C(1)	93.6(1)
C(8)–N–Si	120.3(2)	C(8)–N–Si	121.3(1)
C(8)–N–Ti	139.5(2)	C(8)–N–Zr	132.8(1)
Si–N–Ti	100.1(1)	Si–N–Zr	105.7(1)
C(12)–C(13)–C(14)	126.1(3)	C(12)–C(13)–C(14)	122.1(1)
C(13)–C(14)–C(15)	125.7(2)	C(13)–C(14)–C(15)	124.3(1)
C(14)–C(15)–B	118.6(2)	C(14)–C(15)–B	111.5(1)
C(14)–C(15)–Ti	70.6(1)	C(14)–C(15)–Zr	61.9(1)
Ti–C(15)–H(15A)	73.5	Zr–F(1)–C(17)	151.1(1)
Ti–C(15)–H(15B)	60.7	Zr···C(15)–H(15A)	47.9
Ti–C(15)–B	169.4(2)	Zr···C(15)–B	132.6(1)
C(15)–B–C(16)	115.8(6)	C(15)–B–C(16)	112.7(1)
C(15)–B–C(22)	102.8(2)	C(15)–B–C(22)	102.8(1)
C(15)–B–C(28)	107.0(2)	C(15)–B–C(28)	111.8(1)
C(16)–B–C(22)	112.5(2)	C(16)–B–C(22)	112.2(1)
C(16)–B–C(28)	103.6(2)	C(16)–B–C(28)	104.7(1)
C(22)–B–C(28)	115.5(2)	C(22)–B–C(28)	112.9(1)

<sup>a</sup> Cp(c) designates the centroid of the five-membered cyclopentadienyl ring. <sup>b</sup> M···H distance was calculated on the basis of the H atom being displaced 1.09 Å from C(15).

-135.7, -189.2 (ortho C–F); -156.3, -158.4 (2), -159.2, -161.9, -163.6, -164.0 (2), -165.1 (para and meta C–F). IR ( $\text{cm}^{-1}$ ): 2952(s), 2919(s), 2850(s), 2724(w), 2668(vw), 1641(m), 1513(m), 1459(s), 1376(s), 1366(sh), 1347(s), 1273(m), 1256(m), 1182(w), 1170(w), 1106(w), 1082(m), 1064(w), 1046(w), 975(m), 929(w), 901(w), 834(m), 812(w), 784(m), 757(m), 725(m), 693(w), 678(w). Anal. Calcd for  $\text{C}_{33}\text{H}_{25}\text{NSiBF}_{15}\text{Zr}$ : C, 46.59; H, 2.96; N, 1.65. Found: C, 46.10; H, 3.19; N, 1.65.

**X-ray Structural Analyses of  $[(\text{C}_5\text{H}_4)\text{SiMe}_2(\text{N-t-Bu})]\text{M}^+(\mu\text{-C}_4\text{H}_6)\text{B}^-(\text{C}_6\text{F}_5)_3$ ,  $\text{M} = \text{Ti}, \text{Zr}$ .** A crystal of  $[(\text{C}_5\text{H}_4)\text{SiMe}_2(\text{N-t-Bu})]\text{Ti}^+(\mu\text{-C}_4\text{H}_6)\text{B}^-(\text{C}_6\text{F}_5)_3$  was sealed in a glass capillary tube under a nitrogen atmosphere and then optically aligned on the goniostat of a Siemens P4 automated X-ray diffractometer. The sample was cooled to -50 °C with a LT-2 low-temperature attachment. The reflections used for the unit cell determination were located and indexed by the automatic peak search routine of XSCANS.<sup>23</sup> The lattice parameters and orientation matrix were calculated from a nonlinear least-squares fit of the orientation angles of 39 reflections.

(21) Sekutowski, D. G.; Stucky, G. D. *Inorg. Chem.* **1975**, *14*, 2192.  
(22) Massey, A. G.; Park, A. J. *J. Organomet. Chem.* **1964**, *2*, 245.

(23) XSCANS (version 2.0) is a diffractometer control system developed by Siemens Analytical X-ray Instruments, Madison, WI.

Intensity data were measured with graphite-monochromated Mo K $\alpha$  radiation and variable  $\omega$  scans. Background counts were measured at the beginning and at the end of each scan with the crystal and counter kept stationary. The combined intensities of three standard reflections, which were measured after every 100 reflections, did not show any indication of crystal movement or decay. The raw data were corrected for Lorentz–polarization effects. No absorption correction was applied.

The crystal of [(C<sub>5</sub>H<sub>4</sub>)SiMe<sub>2</sub>(N-t-Bu)]Zr(+)( $\mu$ -C<sub>4</sub>H<sub>6</sub>)B(-)(C<sub>6</sub>F<sub>5</sub>)<sub>3</sub> was coated with 'magic oil' (Lancaster), placed on the end of a glass fiber, and then inserted into the cold nitrogen gas stream held at -75 °C (Oxford Cryosystem series 600 cryostream cooler). The low-temperature X-ray data were collected with a Nonius Kappa CCD diffractometer with Mo K $\alpha$  radiation provided by a rotating anode X-ray generator operating at 5.0 kW with a 0.3  $\times$  0.3 mm focus. The scan frame was 1.0 deg and the integration time per scan was 60 s. Data collection using omega and phi scans was performed with COLLECT (Nonius BV, 1998), data reduction was performed with Denzo-SMN,<sup>24</sup> and an absorption correction (range of transmission factors 0.855–0.942) was performed with SORTAV.<sup>25</sup>

Approximate positional coordinates for all of the non-hydrogen atoms were determined by direct methods and difference Fourier analysis. The isotropic temperature factors for all of the hydrogen atoms were set at 1.2 or 1.5 times that of the adjacent carbon. The positions of the methyl hydrogen atoms were optimized by a rigid rotating group refinement with idealized tetrahedral angles. The lattice of [(C<sub>5</sub>H<sub>4</sub>)SiMe<sub>2</sub>(N-t-Bu)]Zr(+)( $\mu$ -C<sub>4</sub>H<sub>6</sub>)B(-)(C<sub>6</sub>F<sub>5</sub>)<sub>3</sub> contained a 50:50 disordered molecule of toluene, which was modeled by constraining the six carbon atoms of the aryl ring to a hexagon with an edge length of 1.39 Å and restraining the C(methyl)–C(ipso)

and C(methyl)···C(ortho) distances to 1.54  $\pm$  0.02 Å and 2.54  $\pm$  0.02 Å, respectively. Full-matrix least-squares refinement with SHELXL-97 or SHELXTL-NT,<sup>26</sup> based upon the minimization of  $\sum w_i |F_o^2 - F_c^2|^2$  with weighting given by the expression  $w_i^{-1} = [\sigma^2(F_o^2) + (aP)^2 + bP]$  where  $P = (\text{Max}(F_o^2, 0) + 2F_c^2)/3$ , converged to give the values of the final discrepancy indices<sup>27</sup> provided in Table 2. Selected interatomic distances and bond angles are compared in Table 3.

**Acknowledgment.** Financial support for this research was provided by the donors of the Petroleum Research Fund, administered by the American Chemical Society. J.L.P. gratefully acknowledges the support provided by the Chemical Instrumentation Program of the National Science Foundation to acquire an automated X-ray diffractometer at West Virginia University. J.L.P. expresses his appreciation to Professors Hans Reich and Clark Landis of the University of Wisconsin–Madison for helpful discussions and to Birgit Wibbeling, Joachim Strauch, and Gerard Kehr of the University of Münster for their assistance.

**Supporting Information Available:** Complete tables of the results of the X-ray structural analyses performed on [(C<sub>5</sub>H<sub>4</sub>)SiMe<sub>2</sub>(N-t-Bu)]M(+)( $\mu$ -C<sub>4</sub>H<sub>6</sub>)B(-)(C<sub>6</sub>F<sub>5</sub>)<sub>3</sub>, M = Ti, Zr. This material is available free of charge via the Internet at <http://pubs.acs.org>.

OM040057K

(26) SHELXL-97 and SHELXTL-NT were developed by Professor G. Sheldrick, Institut für Anorganische Chemie, University of Göttingen, D-37077, Göttingen, Germany, for single-crystal X-ray structural analyses.

(27) The discrepancy indices were calculated from the expressions  $R1 = \sum |F_o| - |F_c| / \sum |F_o|$  and  $wR2 = [\sum (w_i(F_o^2 - F_c^2)^2) / \sum (w_i(F_o^2)^2)]^{1/2}$ . The standard deviation of an observation of unit weight (GOF) is equal to  $[\sum (w_i(F_o^2 - F_c^2)^2) / (n - p)]^{1/2}$ , where  $n$  is the number of reflections and  $p$  is the number of parameters varied during the last refinement cycle.

(24) Otwinowski, Z.; Minor, W. *Methods Enzymol.* **1997**, *276*, 307.

(25) (a) Blessing, R. H. *Acta Crystallogr., Sect. A* **1995**, *51*, 33. (b) Blessing, R. H. *J. Appl. Crystallogr.* **1997**, *30*, 421.